

# Instability in the Hartmann–Hahn double resonance

Roei Levi, Sergei Masis and Eyal Buks

*Andrew and Erna Viterbi Department of Electrical Engineering, Technion, Haifa 32000, Israel*

(Dated: July 10, 2020)

The Hartmann-Hahn technique allows sensitivity enhancement of magnetic resonance imaging and spectroscopy by coupling the spins under study to another spin species that is externally driven. Here we theoretically study the coupled spins' dynamics, and find that for a certain region of driving parameters the system becomes unstable. The required conditions for making this region of instability becoming experimentally accessible are discussed.

PACS numbers: 76.70.-r, 76.70.Dx

## I. INTRODUCTION

The technique of cross-polarization (CP) [1] is widely employed in magnetic resonance imaging for sensitivity enhancement. Significant CP can be achieved by applying the so-called Hartmann–Hahn double resonance (HHDR) [2]. Near the HHDR magnetization can be efficiently transferred between different spin species [3]. Commonly, CP is implemented to enhance the detection sensitivity of a given spin species under study by applying external driving to another ancilla spin species having higher polarization. When the Rabi frequency of the ancilla spins matches the Larmor frequency of the spins under study the so-called Hartmann–Hahn (HH) matching condition is satisfied [4] [note that this is not the same as the matching condition given by Eq. (4) of Ref. [2]]. In that region a significant CP can be obtained. In thermal equilibrium the initial polarization of the ancilla spins is determined by their gyromagnetic ratio and the temperature [5, 6]. The initial polarization can be further enhanced when the technique of optically-induced spin polarization (OISP) can be applied [7].

Here we theoretically study back-reaction effects near the HHDR. A stability analysis is performed by a linearization of the coupled Bloch equations for the two spins, one of which is externally-driven. We calculate a correction to the effective damping rate of the undriven spin, which is induced by the coupling to the driven one. Analytical results are validated against numerical calculations. A region of instability, inside which the two-spin system is expected to exhibit self-excited oscillation (SEO), is identified. The experimental feasibility of reaching this instability region is discussed. Related effects of Sisyphus cooling, amplification, lasing and SEO have been theoretically predicted in other systems having a similar retarded response [8–13].

## II. DIPOLAR BACK REACTION

Consider two two-level systems (TLS) having a mutual coupling that is characterized by a coupling coefficient  $g$ . The first TLS, which is labelled as 'a', has a relatively low angular frequency  $\omega_{a0}$  in comparison with

the angular frequency  $\omega_{b0}$  of the second TLS, which is labelled as 'b', and which is externally driven. It is assumed that the state of the system can be characterized by the vector of coordinates  $\bar{P} = (P_1, P_2, P_3, P_4, P_5, P_6)^T$ , where  $(P_1, P_2, P_3) = (P_{a+}, P_{a-}, P_{az})$  and  $(P_4, P_5, P_6) = (P_{b+}, P_{b-}, P_{bz})$  are the Bloch vectors of the first and second TLS, respectively. It is further assumed that the vector of coordinates  $\bar{P}$  satisfies a set of coupled Bloch equations [14], which are expressed as

$$\frac{dP_n}{dt} + \Theta_n(\bar{P}) = F_n, \quad (1)$$

where  $n \in \{1, 2, \dots, 6\}$ , the functions  $\Theta_n(\bar{P})$  (to be specified later) are time independent (which is possible provided that a rotating frame is used for the driven TLS) and  $F_n$  represent fluctuating noise terms having vanishing average values. Let  $\bar{P}_0$  be a fixed point, for which  $\Theta_n(\bar{P}_0) = 0$  for all  $n \in \{1, 2, \dots, 6\}$ . Fluctuations around the fixed point are governed by

$$\frac{d\bar{P}'}{dt} + J\bar{P}' = \bar{F}, \quad (2)$$

where the vector of relative coordinates  $\bar{P}' = (P'_1, P'_2, P'_3, P'_4, P'_5, P'_6)^T$  is defined by  $\bar{P}' = \bar{P} - \bar{P}_0$ , the vector of noise terms  $\bar{F}$  is given by  $\bar{F} = (F_1, F_2, F_3, F_4, F_5, F_6)^T$  and the  $6 \times 6$  Jacobian matrix  $J$  at the fixed point  $\bar{P}_0$  is defined by  $J_{m,n} = \partial\Theta_m/\partial P_n$ . The Jacobian matrix  $J$  at the fixed point is expressed in a block form as

$$J = \begin{pmatrix} J_x & gV_{xy} \\ gV_{yx} & J_y \end{pmatrix}. \quad (3)$$

The subspace corresponding to the subscript x (y) is henceforth referred to as the system (ancilla) subspace. For convenience, the system subspace is chosen to be of dimension 2 (corresponding to the transverse variables  $P_{a+}$  and  $P_{a-}$  of spin 'a') and the ancilla subspace of dimension 4 (corresponding to the variables  $P_{az}$ ,  $P_{b+}$ ,  $P_{b-}$  and  $P_{bz}$ ).

Applying the Fourier transform to Eq. (2) yields (Fourier angular frequency is denoted by  $\omega$  and lower case  $f$  and  $p$  denote the Fourier transform of uppercase  $F$  and  $P$  variables, respectively)

$$\begin{pmatrix} J_x - i\omega & gV_{xy} \\ gV_{yx} & J_y - i\omega \end{pmatrix} \begin{pmatrix} \bar{p}_x(\omega) \\ \bar{p}_y(\omega) \end{pmatrix} = \begin{pmatrix} \bar{f}_x(\omega) \\ \bar{f}_y(\omega) \end{pmatrix}, \quad (4)$$

where

$$\begin{aligned}\bar{p}_x(\omega) &= (p_1(\omega), p_1^*(-\omega))^T, \\ \bar{p}_y(\omega) &= (p_3(\omega), p_4(\omega), p_4^*(-\omega), p_6(\omega))^T,\end{aligned}$$

and

$$\begin{aligned}\bar{f}_x(\omega) &= (f_1(\omega), f_1^*(-\omega))^T, \\ \bar{f}_y(\omega) &= (f_3(\omega), f_4(\omega), f_4^*(-\omega), f_6(\omega))^T,\end{aligned}$$

[note that the  $n = 2$  ( $n = 5$ ) equation of (1) is the complex conjugate of the  $n = 1$  ( $n = 4$ ) equation of (1)]. Multiplying the first [second] row of blocks of Eq. (4) by  $\chi_x(\omega) \equiv (J_x - i\omega)^{-1} [\chi_y(\omega) \equiv (J_y - i\omega)^{-1}]$  yields  $\bar{p}_x(\omega) + g\chi_x(\omega) V_{xy}\bar{p}_y(\omega) = \chi_x(\omega) \bar{f}_x(\omega)$  and  $\bar{p}_y(\omega) + g\chi_y(\omega) V_{yx}\bar{p}_x(\omega) = \chi_y(\omega) \bar{f}_y(\omega)$ , and thus  $\bar{p}_x(\omega)$  can be expressed as  $\bar{p}_x(\omega) = \chi_{x,\text{eff}}(\omega) \bar{f}_x(\omega)$ , where  $\chi_{x,\text{eff}}(\omega)$  is given by [the term proportional to  $\bar{f}_y(\omega)$  is disregarded, since it does not affect the expectation value of  $\chi_{x,\text{eff}}(\omega)$ ]

$$\begin{aligned}\chi_{x,\text{eff}}(\omega) &= (1 - g^2\chi_x(\omega) V_{xy}\chi_y(\omega) V_{yx})^{-1} \chi_x(\omega) \\ &= (J_x - i\omega - g^2V_{xy}\chi_y(\omega) V_{yx})^{-1}.\end{aligned}\quad (5)$$

The expression for  $\chi_{x,\text{eff}}(\omega)$  given by Eq. (5) suggests that the coupling effectively shifts the (complex) resonance frequency of the undriven spin (i.e. the first TLS labeled as 'a'). To lowest nonvanishing order in the coupling coefficient  $g$ , the underlying mechanism responsible for this shift, as revealed by Eq. (5), is a three-step feedback process. In the first step, consider the case where spin 'a' undergoes precession with small amplitude at its own Larmor (i.e. resonance) frequency. The term  $gV_{yx}$  in Eq. (5) represents the driving applied to the ancilla system due to the precession of spin 'a', and the term  $\chi_y(\omega)$  in Eq. (5) represents the corresponding response of the ancilla to this driving (the second step). This response of the ancilla gives rise to a feedback driving applied to spin 'a' occurring in the third step, where the feedback coupling is represented by the term  $gV_{xy}$  in Eq. (5).

The coupling-induced feedback driving applied to spin 'a' can be expressed as a sum of two orthogonal quadratures, both oscillating at the Larmor frequency of spin 'a'. The first one is in-phase with the precession of spin 'a', and the second one, which occurs due to retardation in the response of the ancilla to the precession of spin 'a', is out of phase. The in-phase quadratures gives rise to a change in the real part of the effective resonance frequency of the undriven spin 'a' (i.e. a change in its effective Larmor frequency), whereas the change in the effective damping rate is proportional to the amplitude of the out of phase quadrature.

In general, dipolar interaction is represented by a Hamiltonian  $\mathcal{H}_d$  containing terms proportional to operators having the form  $S_{a,i}S_{b,j}$ , where  $S_{a,i}$  ( $S_{b,j}$ ) is the  $i$ 'th ( $j$ 'th) component of spin 'a' ('b') angular momentum operator  $\mathbf{S}_a$  ( $\mathbf{S}_b$ ) (see [3] p. 66). Terms proportional to the longitudinal component of  $\mathbf{S}_a$  are disregarded since they do not contribute to effective driving at the Larmor

frequency of spin 'a'. Moreover, terms proportional to transverse components of  $\mathbf{S}_b$  can be disregarded as well, provided that the Larmor frequency of spin 'b' is much higher than the Larmor frequency of spin 'a'. In this limit the driving applied to spin 'b' due to the precession of spin 'a' can be considered as slow, and consequently its transverse component has a weak effect compared to the effect of its longitudinal component (which effectively modulates the Larmor frequency of spin 'b'). When only dominant terms are kept the dipolar coupling Hamiltonian  $\mathcal{H}_d$  becomes  $\mathcal{H}_d = 2g\hbar^{-1}(S_{a+} + S_{a-})S_{bz}$ .

The Hamiltonian  $\mathcal{H}$  of the closed system is given by

$$\mathcal{H} = \omega_{a0}S_{az} + \omega_{b0}S_{bz} + \omega_{b1}(S_{b+} + S_{b-}) + \mathcal{H}_d, \quad (6)$$

where the driving amplitude and angular frequency are denoted by  $\omega_{b1}$  and  $\omega_p = \omega_{b0} + \Delta_b$ , respectively ( $\Delta_b$  is the driving detuning), the operators  $S_{a\pm}$  are given by  $S_{a\pm} = S_{ax} \pm iS_{ay}$ , and the rotated operators  $S_{b\pm}$  are given by  $S_{b\pm} = (S_{bx} \pm iS_{by})e^{\mp i\omega_p t}$ . The Heisenberg equation of motion  $dO/dt = -i\hbar^{-1}[O, \mathcal{H}] + \partial O/\partial t$ , where  $O$  is a given observable, together with the spin commutation relations  $[S_z, S_{\pm}] = \pm\hbar S_{\pm}$  and  $[S_+, S_-] = 2\hbar S_z$  yield (overdot denotes a time derivative)  $\dot{S}_{a+} - i\omega_{a0}S_{a+} + 4ig\hbar^{-1}S_{az}S_{bz} = 0$ ,  $\dot{S}_{az} + 2ig\hbar^{-1}(S_{a+} - S_{a-})S_{bz} = 0$ ,  $\dot{S}_{b+} + i(\Delta_b - 2g\hbar^{-1}(S_{a+} + S_{a-}))S_{b+} + 2i\omega_{b1}S_{bz} = 0$  and  $\dot{S}_{bz} + i\omega_{b1}(S_{b+} - S_{b-}) = 0$ .

The interaction with the environment is accounted for by assuming that the closed system is weakly coupled to thermal baths at thermal equilibrium. The coupling turns the deterministic equations of motion for the spin operators into Langevin equations containing both damping and fluctuating terms. By applying thermal averaging, which is denoted by  $\langle \rangle$ , a set of coupled equations can be derived.

The coupling terms (i.e. the terms proportional to  $g$ ) in the above-derived evolution equations for the operators  $S_{a+}$  and  $S_{b+}$  are proportional to operators having the form  $AB$ , where  $A$  ( $B$ ) is an operator of spin 'a' ('b'). The following holds  $\langle AB \rangle = \langle A \rangle \langle B \rangle + \langle V_{AB} \rangle$ , where  $V_{AB} = (A - \langle A \rangle)(B - \langle B \rangle)$ . In the mean field approximation the term  $\langle V_{AB} \rangle$  is disregarded. This approximation greatly simplifies the problem, since it allows the description of the dynamics in terms of the vector  $\vec{P} = (P_{a+}, P_{a-}, P_{az}, P_{b+}, P_{b-}, P_{bz})^T$ , where  $(\hbar/2)P_{az} = \langle S_{az} \rangle$ ,  $(\hbar/2)P_{bz} = \langle S_{bz} \rangle$ ,  $\hbar P_{a\pm} = \langle S_{a\pm} \rangle$  and  $\hbar P_{b\pm} = \langle S_{b\pm} \rangle$ . The vector  $\vec{P}$  is determined by 2 real numbers  $P_{az}$  and  $P_{bz}$ , and 2 complex numbers  $P_{a+} = P_{a-}^*$  and  $P_{b+} = P_{b-}^*$ , whereas more variables are needed for treating the general case (the density operator of a two-spin system is determined by 15 real numbers). Note that for product states, for which  $\langle V_{AB} \rangle = 0$ , the mean field approximation becomes exact. It can be used provided that the lifetime of entangled states is much shorter than all single spin lifetimes. When this assumption cannot be made a more general analysis, which does not exclude entanglement, is needed.

In the mean field approximation the functions

$\overline{\Theta}(\bar{P}) = (\Theta_1, \Theta_2, \Theta_3, \Theta_4, \Theta_5, \Theta_6)^T$  are given by  $\Theta_1 = \Theta_2^* = (\gamma_{a2} - i\omega_{a0})P_{a+} + igP_{az}P_{bz}$ ,  $\Theta_3 = \gamma_{a1}(P_{az} - P_{az,s}) + 2ig(P_{a+} - P_{a-})P_{bz}$ ,  $\Theta_4 = \Theta_5^* = (\gamma_{b2} + i\Delta_b)P_{b+} + i\omega_{b1}P_{bz} - 2ig(P_{a+} + P_{a-})P_{b+}$  and  $\Theta_6 = \gamma_{b1}(P_{bz} - P_{bz,s}) + 2i\omega_{b1}(P_{b+} - P_{b-})$ , where  $\gamma_{a1}$  ( $\gamma_{b1}$ ) is the longitudinal relaxation rate of the undriven (driven) spin,  $\gamma_{a2}$  ( $\gamma_{b2}$ ) is the transverse relaxation rate of the undriven (driven) spin,  $P_{az,s} = -\tanh(\hbar\omega_{a0}/2k_B T)$  ( $P_{bz,s} = -\tanh(\hbar\omega_{b0}/2k_B T)$ ) is the value of  $P_{az}$  ( $P_{bz}$ ) in thermal equilibrium,  $k_B$  is the Boltzmann's constant and  $T$  is the temperature. Note that in steady state the expectation values of the transverse components of the undriven spin 'a' vanish (for the decoupled case  $g = 0$ ), i.e.  $P_{a+} = P_{a-} = 0$ .

The derivation below is mainly devoted to the analytical inversion of the matrix  $J_y - i\omega$ , which, in turn, allows the evaluation of  $\chi_{x,\text{eff}}(\omega)$  according to Eq. (5). The matrices  $J_x$  ( $2 \times 2$ ) and  $J_y$  ( $4 \times 4$ ) are given by

$$J_x = \begin{pmatrix} \gamma_{a2} - i\omega_{a0} & 0 \\ 0 & \gamma_{a2} + i\omega_{a0} \end{pmatrix}, \quad (7)$$

$$J_y = \begin{pmatrix} \gamma_{a1} & 0 & 0 & 0 \\ 0 & \gamma_{b2} + i\Delta_b & 0 & i\omega_{b1} \\ 0 & 0 & \gamma_{b2} - i\Delta_b & -i\omega_{b1} \\ 0 & 2i\omega_{b1} & -2i\omega_{b1} & \gamma_{b1} \end{pmatrix}, \quad (8)$$

and the coupling matrices  $V_{xy}$  ( $2 \times 4$ ) and  $V_{yx}$  ( $4 \times 2$ ) are given by

$$V_{xy} = \begin{pmatrix} iP_{bz} & 0 & 0 & iP_{az} \\ -iP_{bz} & 0 & 0 & -iP_{az} \end{pmatrix}, \quad (9)$$

$$V_{yx} = \begin{pmatrix} 2iP_{bz} & -2iP_{bz} \\ -2iP_{b+} & -2iP_{b+} \\ 2iP_{b-} & 2iP_{b-} \\ 0 & 0 \end{pmatrix}. \quad (10)$$

To lowest nonvanishing order in  $g$  the blocks  $V_{xy}$  and  $V_{yx}$  are evaluated by replacing all variables  $\bar{P}$  by their averaged steady-state values in the absence of coupling, which are denoted as  $\bar{P}_0 = (P_{a+0}, P_{a-0}, P_{az0}, P_{b+0}, P_{b-0}, P_{bz0})$ . These averaged steady-state values are evaluated in appendix A, and it is found that [see Eq. (A9)]

$$P_{bz0} = \frac{\left(1 + \frac{\Delta_b^2}{\gamma_{b2}^2}\right)P_{bz,s}}{1 + \frac{4\omega_{b1}^2}{\gamma_{b1}\gamma_{b2}} + \frac{\Delta_b^2}{\gamma_{b2}^2}}, \quad (11)$$

$$P_{b+0} = \frac{\frac{\omega_{b1}}{\gamma_{b2}}\left(-\frac{\Delta_b}{\gamma_{b2}} - i\right)P_{bz,s}}{1 + \frac{4\omega_{b1}^2}{\gamma_{b1}\gamma_{b2}} + \frac{\Delta_b^2}{\gamma_{b2}^2}}, \quad (12)$$

$P_{b+0}^* = P_{b-0}$ ,  $P_{az0} = P_{az,s}$  and  $P_{a+0} = P_{a-0} = 0$  (since the first spin is not driven).

Next, the effective susceptibility matrix  $\chi_{x,\text{eff}}(\omega)$  is evaluated at the resonance frequency of the first TLS  $\omega_{a0}$ . The following holds [see Eq. (8)]

$$\chi_y(\omega_{a0}) = (J_y - i\omega_{a0})^{-1} = \frac{1}{D_L} \begin{pmatrix} \frac{D_L}{D_0} & 0 & 0 & 0 \\ 0 & D_2D_3 + 2\omega_{b1}^2 & 2\omega_{b1}^2 & -i\omega_{b1}D_2 \\ 0 & 2\omega_{b1}^2 & D_1D_3 + 2\omega_{b1}^2 & i\omega_{b1}D_1 \\ 0 & -2i\omega_{b1}D_2 & 2i\omega_{b1}D_1 & D_1D_2 \end{pmatrix}, \quad (13)$$

where  $D_0 = \gamma_{a1} - i\omega_{a0}$ ,  $D_1 = \gamma_{b2} + i\Delta_b - i\omega_{a0}$ ,  $D_2 = \gamma_{b2} - i\Delta_b - i\omega_{a0}$ ,  $D_3 = \gamma_{b1} - i\omega_{a0}$  and  $D_L = D_1D_2D_3 + 2\omega_{b1}^2(D_1 + D_2)$ . As can be seen from Eq. (5), only the diagonal elements of  $V_{xy}\chi_y(\omega)V_{yx}$  contribute to the eigenvalues of  $\chi_{x,\text{eff}}(\omega)$  to lowest nonvanishing order in  $g$  (second order). To the same order the effective complex frequency of the first TLS is  $\omega_{a0} + i\gamma_{a2} - i\Upsilon_a$ , where

$$\Upsilon_a = g^2(V_{xy}\chi_y(\omega)V_{yx})_{11}. \quad (14)$$

Substituting the corresponding coupling matrices  $V_{xy}$  and  $V_{yx}$  leads to [see Eqs. (9), (10), (13) and (12)]

$$\Upsilon_a = -2g^2 \left( \frac{P_{bz0}^2}{D_0} + 2i\omega_{b1}P_{az0} \frac{D_2P_{b+0} + D_1P_{b-0}}{D_L} \right). \quad (15)$$

The determinant  $D_L$  can be expressed as  $D_L/\omega_{a0}^3 = (\gamma_{b1}/\omega_{a0})\eta$ , where  $\eta = \eta' + i\eta''$ ,  $\eta' = \Delta_b^2/\omega_{a0}^2 - (1 + (2\gamma_{b2}/\gamma_{b1})(1 - 2\omega_{b1}^2/\omega_{a0}^2) - \gamma_{b2}^2/\omega_{a0}^2)$ ,  $\eta'' = (1 - (2\gamma_{b1}/\omega_{a0} + \gamma_{b2}/\omega_{a0})(\gamma_{b2}/\omega_{a0}) - \omega_R^2/\omega_{a0}^2)/(\gamma_{b1}/\omega_{a0})$ , and  $\omega_R$ , which is given by

$$\omega_R = \sqrt{4\omega_{b1}^2 + \Delta_b^2}, \quad (16)$$

is the Rabi frequency of the driven spins, thus Eq. (15) can be rewritten as

$$\frac{\omega_{a0}\Upsilon_a}{2g^2} = \frac{\frac{4(1 + \frac{2i\gamma_{b2}}{\omega_{a0}})\Delta_b\omega_{b1}^2P_{az,s}P_{bz,s}}{\gamma_{b2}^2\gamma_{b1}\eta}}{1 + \frac{4\omega_{b1}^2}{\gamma_{b1}\gamma_{b2}} + \frac{\Delta_b^2}{\gamma_{b2}^2}} + \frac{\left(1 + \frac{\Delta_b^2}{\gamma_{b2}^2}\right)\left(\frac{\gamma_{a1}}{\omega_{a0}} - i\right)P_{bz,s}^2}{\left(1 + \frac{4\omega_{b1}^2}{\gamma_{b1}\gamma_{b2}} + \frac{\Delta_b^2}{\gamma_{b2}^2}\right)^2\left(1 + \frac{\gamma_{a1}^2}{\omega_{a0}^2}\right)}. \quad (17)$$

The effective damping rate of spin 'a' is given by  $\gamma_{a2}(1 + \alpha_a)$ , where  $\alpha_a = -\text{Re}(\Upsilon_a)/\gamma_{a2}$ . The contribution of the term in the second line of Eq. (17) to  $\alpha_a$  can be disregarded provided that  $\gamma_{a1} \ll \omega_{a0}$ .

The dependence according to Eq. (17) of  $\alpha_a$  on the normalized detuning  $\Delta_b/\omega_{a0}$  and on the normalized driving amplitude  $\omega_{b1}/\omega_{a0}$  is shown in Fig. 1(a) (the term proportional to  $P_{bz0}^2$  is disregarded since it is assumed that  $\gamma_{a1} \ll \omega_{a0}$ ). The parameters that have been used for generating the plot are listed in the figure caption. Spin 'b' is assumed to be fully polarized, for instance by OISP.

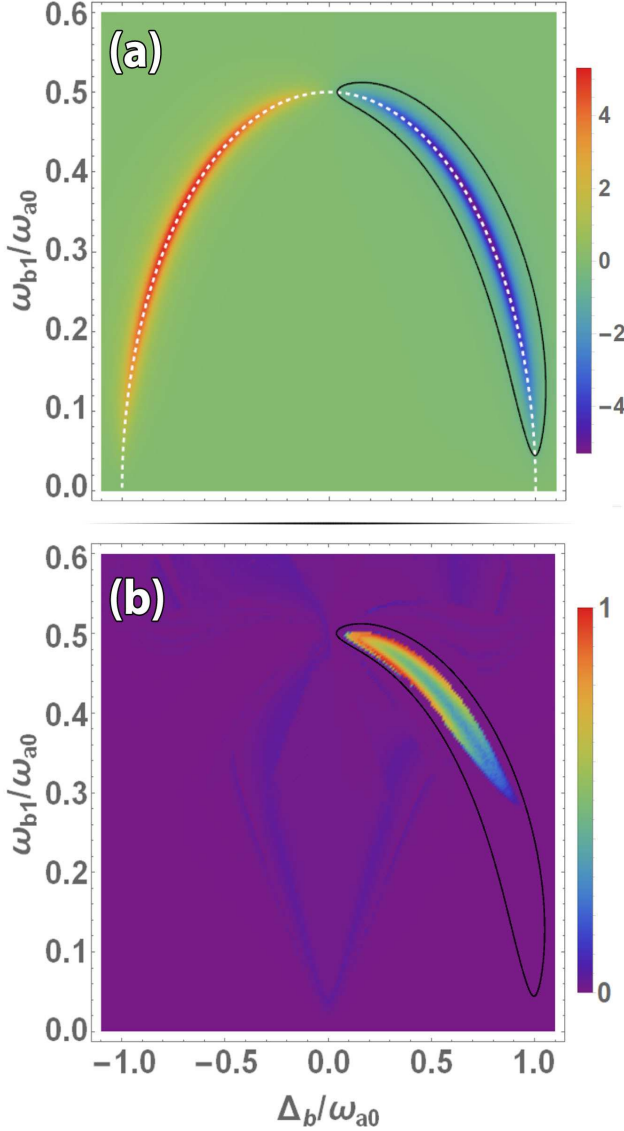


FIG. 1: The effective damping rate of spin 'a'. (a) Color-coded plot of  $\alpha_a$  vs.  $\Delta_b/\omega_{a0}$  and  $\omega_{b1}/\omega_{a0}$  with parameters  $g/\omega_{a0} = 1.0$ ,  $\gamma_{a1}/\omega_{a0} = 10^{-2}$ ,  $\gamma_{a2}/\omega_{a0} = 10^{-4}$ ,  $\gamma_{b1}/\omega_{a0} = 3.7 \times 10^{-3}$ ,  $\gamma_{b2}/\omega_{a0} = 3.7 \times 10^{-2}$ ,  $P_{az,s} = -5 \times 10^{-4}$  and  $P_{bz,s} = -1$ . (b) Numerical solution for the normalized steady state amplitude of  $P_{a+}$  vs.  $\Delta_b/\omega_{a0}$  and  $\omega_{b1}/\omega_{a0}$ , with the same parameters as in (a). The fluctuating noise terms  $\bar{F}$  are disregarded in the numerical calculation.

Also, the curve along which  $\alpha_a = -1$  is shown as a solid black curve on the same plot. This curve labels the border between the regions of positive and negative effective damping rates for the undriven spin. When the driving is red-detuned, i.e. when  $\Delta_b$  is negative, the change in damping rate  $\gamma_{a2}$  is positive, and consequently spin cooling is expected to occur [15]. The opposite behavior occurs with blue detuning, i.e. when  $\Delta_b$  is positive. Specifically, SEO is expected in the area enclosed by the black curve. Along this curve the system undergoes a

Hopf bifurcation [16].

For both red and blue detuning, large change in the effective spin damping rate occurs near the overlaid dashed white line in Fig. 1, along which the Rabi frequency  $\omega_R$  coincides with  $\omega_{a0}$ , i.e.  $\Delta_b = \pm \sqrt{\omega_{a0}^2 - 4\omega_{b1}^2}$ , and the HH matching condition is satisfied. This behavior can be explained by noticing that  $|\eta''| \ll 1$  along the dashed line, i.e. when  $\omega_R = \omega_{a0}$ , and consequently  $|\alpha_a|$  obtains a peak.

The underlying mechanism responsible for the change in the effective damping rate of the undriven spin is similar to a related mechanism occurring in optomechanical cavities [15]. The change in the effective damping rate of the system under study (i.e. spin 'a') is attributed to the retardation in the response of the driven ancilla (i.e. spin 'b') to fluctuation in the state of spin 'a'. Both effects of cooling and heating are attributed to imbalance between fluctuation and dissipation [15] occurring due to the change in the effective damping rate of spin 'a'.

The analytic result given by Eq. (17) was validated against a numerical simulation of a time dependent solution of the equations of motion [see Eq. (1)]. A plot for the normalized steady state amplitude of  $P_{a+}$  vs. the normalized detuning  $\Delta_b/\omega_{a0}$  and the normalized driving amplitude  $\omega_{b1}/\omega_{a0}$  is shown in Fig. 1(b). The undriven spin experiences SEO in the region of negative effective damping rate (encircled by the black curve). Deviation between the region of SEO that is obtained by the solid black curve and the one that is obtained from the numerical calculation is attributed to the term  $P_{bz0}^2/D_0$  that was neglected in Eq. (17).

### III. EXPERIMENTAL FEASIBILITY

The experimental feasibility to reach the instability threshold occurring when  $\alpha_a = -1$  is discussed below. Consider the case where the HH condition  $\omega_R = \omega_{a0}$  is satisfied [see the dashed white curve in Fig. 1(a)]. As is demonstrated by Fig. 1, the largest change in  $\alpha_a$  typically occurs when the detuning  $|\Delta_b|$  and driving amplitude  $\omega_{b1}$  are of the same order of magnitude (i.e.  $|\Delta_b| \simeq \omega_{b1} \simeq \omega_{a0}$ ). When the following holds  $\omega_{a0} \ll \omega_{b0}$ ,  $\gamma_{b1} \ll \gamma_{b2} \ll |\Delta_b|$  and  $|\Delta_b| \simeq \omega_{b1} \simeq \omega_{a0}$ , the threshold condition  $\alpha_a = -1$  yields the requirement  $\kappa P_{az,s} P_{bz,s} \simeq 1$ , where  $\kappa = g^2 \gamma_{b1} / (\gamma_{a2} \gamma_{b2}^2)$  is the cooperativity parameter [see Eq. (17)].

As an example, consider two nearby defects in a diamond lattice [17]. The first one having Larmor angular frequency  $\omega_{a0}$  is a negatively charged nitrogen vacancy ( $NV^-$ ) defect [18], and the second one is a nitrogen substitutional defect (P1) [19] having Larmor angular frequency  $\omega_{b0}$ . An externally applied magnetic field  $B$  parallel to the NV axis can be used to tune both  $\omega_{a0}$  and  $\omega_{b0}$ . Two spin states belonging to the  $NV^-$  spin triplet ground state become nearly degenerate near the magnetic field value of  $B = 102$  mT. In that region the angular frequency  $\omega_{b0}$  of the electronic-like P1



transitions is about  $\omega_{b0} = \gamma_e B = 2\pi \times 2.9 \text{ GHz}$ , where  $\gamma_e = 2\pi \times 28.03 \text{ GHz T}^{-1}$  is the electron spin gyromagnetic ratio. For this value of  $\omega_{b0}$  the P1 electronic spin defects can be nearly fully polarized, i.e.  $|P_{bz,s}| \simeq 1$ , by cooling down the sample well below a temperature of about 0.07 K.

In practice, the value of the NV transition frequency  $\omega_{a0}$  (which can be tuned by the externally applied magnetic field) is limited due to the HH matching condition by the maximum possible value of the driving amplitude  $\omega_{b1}$  that can be experimentally achieved. For the case where a high quality factor microwave resonator is employed for driving the P1 spins [13], a value of about  $\omega_{a0} = \omega_R \simeq 2\pi \times 50 \text{ MHz}$ , is reachable. This value is too small to allow making  $|P_{az,s}|$  becoming of order unity using cooling only. However the condition  $|P_{az,s}| \simeq 1$  can be satisfied using the technique of OISP [20, 21].

The dipolar coupling coefficient  $g$  between the NV<sup>-</sup> electron spin and the P1 electron spin is given by  $g/2\pi \simeq 3.6 \text{ GHz} (r_d/a_d)^{-3}$  [3], where  $r_d$  is the NV<sup>-</sup>-P1 distance,  $a_d = 3.57 \text{ \AA}$  is the lattice constant of diamond, and it is assumed for simplicity that the angle between the line joining the two defects and the NV axis vanishes. When both spins are fully polarized and for the typical values of  $\gamma_{a2} = \gamma_{b2} = 2\pi \times 0.1 \text{ MHz}$ ,  $\gamma_{b1} = 2\pi \times 0.01 \text{ MHz}$ , the threshold condition  $\alpha_a = -1$  is satisfied when  $r_d \simeq 8 \text{ nm}$ .

In the above example the case of dipolar coupling between two electron spins localized near different lattice sites was considered. This coupling, however, depends on the distance between sites, and consequently, its study is difficult using measurements of ensembles containing many spins. Such Inhomogeneity is avoided for the case where the same lattice site hosts both spins. For that case spin 'a' is assumed to be a nuclear spin and spin 'b' is an electron spin. For example, for the case of P1 defects in diamond, the dipolar coupling between the nitrogen 14 nuclear spin  $S = 1$  and the spin of the localized unpaired electron occupying the same lattice site gives rise to hyperfine splitting on the order of 100 MHz [13]. Such a coupling is sufficiently strong to make the region of SEO experimentally accessible, and the study of this instability can be performed using measurements of ensembles containing many P1 defects.

#### IV. SUMMARY

Our results demonstrate that a significant change in the effective value of transverse spin relaxation rate can be induced, provided that the HH matching condition can be satisfied. Red-detuned driving provides a positive contribution to the relaxation rate, whereas negative contribution can be obtained by blue-detuned driving. For the former case this effect can be utilized for cooling down spins, while the later case of blue detuning may allow inducing SEO. Operating close to the threshold of SEO, i.e. close to the point where the total effective damping vanishes, may be useful for sensing applications, since

the system is expected to become highly responsive to external perturbations near the threshold.

This work was supported by the Israel Science Foundation and the Security Research Foundation at Technion.

#### Appendix A: Fixed points of Bloch equations

The dynamics of the polarization vector  $\mathbf{P} = P_x \hat{\mathbf{x}} + P_y \hat{\mathbf{y}} + P_z \hat{\mathbf{z}}$ , which describes the state of the spin system, is governed by the Bloch equations [3]

$$\frac{d\mathbf{P}}{dt} = \mathbf{P} \times \boldsymbol{\Omega} + \boldsymbol{\gamma}, \quad (\text{A1})$$

where  $\boldsymbol{\Omega}(t)$  is the rotation vector, which is proportional to the externally applied magnetic field vector (the factor of proportionality is called the gyromagnetic ratio). The vector

$$\boldsymbol{\gamma} = -\gamma_2 P_x \hat{\mathbf{x}} - \gamma_2 P_y \hat{\mathbf{y}} - \gamma_1 (P_z - P_{z,s}) \hat{\mathbf{z}} \quad (\text{A2})$$

represents the contribution of damping, where  $\gamma_1 = 1/T_1$  and  $\gamma_2 = 1/T_2$  are the longitudinal and transverse relaxation rates, respectively, and where  $P_{z,s}$  is the equilibrium steady state polarization.

Consider the case where the rotation vector  $\boldsymbol{\Omega}(t)$  is taken to be given by

$$\boldsymbol{\Omega}(t) = 2\omega_1 (\cos(\omega t) \hat{\mathbf{x}} + \sin(\omega t) \hat{\mathbf{y}}) + \omega_0 \hat{\mathbf{z}}, \quad (\text{A3})$$

where  $\omega_1$ ,  $\omega$  and  $\omega_0$  are real constants. For this case Eq. (A1) becomes

$$\frac{d\mathbf{P}}{dt} + M_B \mathbf{P} = \begin{pmatrix} 0 \\ 0 \\ \gamma_1 P_{z,s} \end{pmatrix}, \quad (\text{A4})$$

where

$$M_B = \begin{pmatrix} \gamma_2 & -\omega_0 & 2\omega_1 \sin(\omega t) \\ \omega_0 & \gamma_2 & -2\omega_1 \cos(\omega t) \\ 2\omega_1 \sin(\omega t) & -2\omega_1 \cos(\omega t) & \gamma_1 \end{pmatrix}. \quad (\text{A5})$$

The variable transformation

$$\begin{pmatrix} P_x \\ P_y \\ P_z \end{pmatrix} = \begin{pmatrix} e^{i\omega t} & e^{-i\omega t} \\ -ie^{i\omega t} & ie^{-i\omega t} \end{pmatrix} \begin{pmatrix} P_+ \\ P_- \end{pmatrix}, \quad (\text{A6})$$

leads to

$$\frac{d}{dt} \begin{pmatrix} P_+ \\ P_- \\ P_z \end{pmatrix} + J \begin{pmatrix} P_+ \\ P_- \\ P_z \end{pmatrix} = \begin{pmatrix} 0 \\ 0 \\ \gamma_1 P_{z,s} \end{pmatrix}, \quad (\text{A7})$$

where

$$J = \begin{pmatrix} \gamma_2 - i\Delta & 0 & i\omega_1 \\ 0 & \gamma_2 + i\Delta & -i\omega_1 \\ 2i\omega_1 & -2i\omega_1 & \gamma_1 \end{pmatrix}, \quad (\text{A8})$$

and where  $\Delta = \omega - \omega_0$  is the driving detuning. The steady state solution of Eq. (A7) is given by

$$\begin{pmatrix} P_{+0} \\ P_{-0} \\ P_{z0} \end{pmatrix} = J^{-1} \begin{pmatrix} 0 \\ 0 \\ \gamma_1 P_{z,s} \end{pmatrix} = \begin{pmatrix} \frac{\frac{\omega_1}{\gamma_2} \left( -\frac{\Delta}{\gamma_2} - i \right)}{1 + \frac{4\omega_1^2}{\gamma_1 \gamma_2} + \frac{\Delta^2}{\gamma_2^2}} \\ \frac{\frac{\omega_1}{\gamma_2} \left( -\frac{\Delta}{\gamma_2} + i \right)}{1 + \frac{4\omega_1^2}{\gamma_1 \gamma_2} + \frac{\Delta^2}{\gamma_2^2}} \\ \frac{1 + \frac{\Delta^2}{\gamma_2^2}}{1 + \frac{4\omega_1^2}{\gamma_1 \gamma_2} + \frac{\Delta^2}{\gamma_2^2}} \end{pmatrix} P_{z,s} . \quad (\text{A9})$$

- 
- [1] A. Pines, M. G. Gibby, and J. S. Waugh, “Proton-enhanced NMR of dilute spins in solids”, *The Journal of Chemical Physics*, pp. 569–590, 1973.
- [2] SR Hartmann and EL Hahn, “Nuclear double resonance in the rotating frame”, *Physical Review*, vol. 128, no. 5, pp. 2042, 1962.
- [3] Charles P Slichter, *Principles of magnetic resonance*, vol. 1, Springer Science & Business Media, 2013.
- [4] Pengcheng Yang, Martin B Plenio, and Jianming Cai, “Dynamical nuclear polarization using multi-colour control of color centers in diamond”, *EPJ Quantum Technology*, vol. 3, pp. 1–9, 2016.
- [5] A Abragam and WG Proctor, “Spin temperature”, *Physical Review*, vol. 109, no. 5, pp. 1441, 1958.
- [6] Anatole Abragam, *The principles of nuclear magnetism*, Number 32. Oxford university press, 1961.
- [7] Paz London, J Scheuer, J-M Cai, I Schwarz, A Retzker, MB Plenio, M Katagiri, T Teraji, S Koizumi, J Isoya, et al., “Detecting and polarizing nuclear spins with double resonance on a single electron spin”, *Physical review letters*, vol. 111, no. 6, pp. 067601, 2013.
- [8] R Glenn and ME Raikh, “Rabi-vibronic resonance with large number of vibrational quanta”, *Physical Review B*, vol. 84, no. 19, pp. 195454, 2011.
- [9] M Grajcar, SHW Van der Ploeg, A Izmalkov, E Ilichev, H-G Meyer, A Fedorov, A Shnirman, and Gerd Schön, “Sisyphus cooling and amplification by a superconducting qubit”, *Nature physics*, vol. 4, no. 8, pp. 612–616, 2008.
- [10] JM De Voogd, JJJ Wagenaar, and TH Oosterkamp, “Dissipation and resonance frequency shift of a resonator magnetically coupled to a semiclassical spin”, *Scientific reports*, vol. 7, pp. 42239, 2017.
- [11] Lior Ella and Eyal Buks, “Hopf bifurcation in a flux qubit coupled to a nanomechanical oscillator”, *arXiv:1210.6902*, 2012.
- [12] Tomás Ramos, Vivishek Sudhir, Kai Stannigel, Peter Zoller, and Tobias J Kippenberg, “Nonlinear quantum optomechanics via individual intrinsic two-level defects”, *Physical review letters*, vol. 110, no. 19, pp. 193602, 2013.
- [13] Hui Wang, Sergei Masis, Roei Levi, Oleg Shtempluk, and Eyal Buks, “Off-resonance coupling between a cavity mode and an ensemble of driven spins”, *Physical Review A*, vol. 95, no. 5, pp. 053853, 2017.
- [14] I Solomon, “Relaxation processes in a system of two spins”, *Physical Review*, vol. 99, no. 2, pp. 559, 1955.
- [15] Markus Aspelmeyer, Tobias J Kippenberg, and Florian Marquardt, “Cavity optomechanics”, *Reviews of Modern Physics*, vol. 86, no. 4, pp. 1391, 2014.
- [16] Brian D Hassard, BD Hassard, Nicholas D Kazarinoff, Y-H Wan, and Y Wah Wan, *Theory and applications of Hopf bifurcation*, vol. 41, CUP Archive, 1981.
- [17] Nir Alfasi, Sergei Masis, Oleg Shtempluk, and Eyal Buks, “Detection of paramagnetic defects in diamond using off-resonance excitation of nv centers”, *Phys. Rev. B*, vol. 99, pp. 214111, Jun 2019.
- [18] Marcus W Doherty, Neil B Manson, Paul Delaney, Fedor Jelezko, Jörg Wrachtrup, and Lloyd CL Hollenberg, “The nitrogen-vacancy colour centre in diamond”, *Physics Reports*, vol. 528, no. 1, pp. 1–45, 2013.
- [19] RJ Cook and DH Whiffen, “Electron nuclear double resonance study of a nitrogen centre in diamond”, *Proceedings of the Royal Society of London A: Mathematical, Physical and Engineering Sciences*, vol. 295, no. 1441, pp. 99–106, 1966.
- [20] Lucio Robledo, Hannes Bernien, Toeno van der Sar, and Ronald Hanson, “Spin dynamics in the optical cycle of single nitrogen-vacancy centres in diamond”, *New Journal of Physics*, vol. 13, no. 2, pp. 025013, 2011.
- [21] DA Redman, S Brown, RH Sands, and SC Rand, “Spin dynamics and electronic states of n-v centers in diamond by epr and four-wave-mixing spectroscopy”, *Physical review letters*, vol. 67, no. 24, pp. 3420, 1991.